Nanoscale

Accepted Manuscript

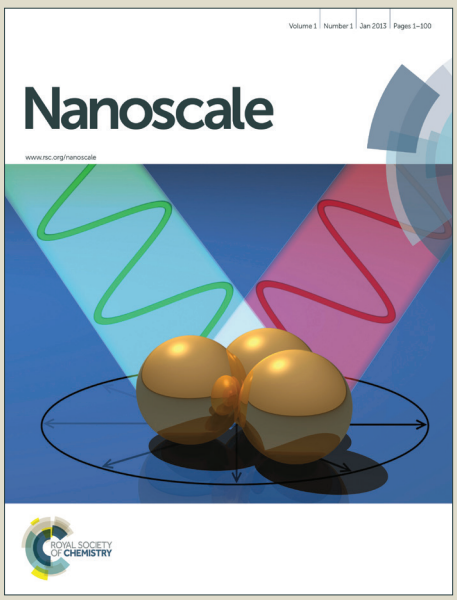

ROYAL SOCIETY OF CHEMISTRY

www.rsc.org/nanoscale

Enhanced photoelectrochemical water splitting performance on TiO_2 nanotube arrays coated with an ultrathin Nitrogen-doped carbon film by molecular layer deposition

Xili Tong, [†,*] *Peng Yang,* [†] *Yunwei Wang,* [†] *Yong Qin,* [†,*] *and Xiangyun Guo* [†]

[†]State Key Laboratory of Coal Conversion, Institute of Coal Chemistry, Chinese Academy of Sciences, Taiyuan, 030001, P. R. China.

[*]Corresponding Author: tongxili@sxicc.ac.cn; Fax: +86351 4040468;

qinyong@sxicc.ac.cn; Fax: +86351 4040081;

ABSTRACT: Vertically oriented TiO_2 nanotube arrays (TNTAs) were conformally coated with an ultrathin Nitrogen-doped (N-doped) carbon film via the carbonization of a polyimide film deposited by molecular layer deposition and simultaneously hydrogenated, thereby creating a core/shell nanostructure with a precisely controllable shell thickness. The core/shell nanostructure provides larger heterojunction interface to substantially reduce the recombination of photogenerated electron-hole pairs, and hydrogenation enhances solar absorption of TNTAs. In addition, the N-doped carbon film coating acts as a high catalytic active surface for oxygen evolution reaction, as well as a protective film to prevent hydrogen-treated TiO_2 nanotubes oxidation by electrolyte or air. As a result, the N-doped carbon film coated TNTAs displayed remarkably improved photocurrent and photostability The TNTAs with a N-doped carbon film of ~1 nm produces a current density of 3.6 $mAcm^{-2}$ at 0 V vs. Ag/AgCl under the illumination of

AM 1.5G (100 $mWcm^{-2}$), which represents one of the highest values achieved with modified TNTAs. Therefore, we propose that ultrathin N-doped carbon film coating on materials is a viable approach to enhance their PEC water splitting performance.

KEYWORDS: TiO_2 Nanotubes · photoanode · carbon film· water splitting· molecular layer deposition

Solar radiation is a renewable energy source that has the capacity to meet global energy demands in a carbon-neutral fashion. Photoelectrochemical (PEC) water splitting, first reported by Fujishima and Honda, [1] is wildly considered as a most promising and appealing approach for large-scale production of hydrogen to supply clean energy using solar energy.[2,3] The PEC cells are typically designed with metal oxide semiconductors as the photoelectrode and noble metals as the auxiliary electrode. Currently, n-type vertically oriented TiO_2 nanotube arrays (TNTAs) fabricated by electrochemical anodization remains a competitive candidate for the state-of-the-art photoanode due to their high level of controllable aspect ratio, high surface area for the sufficient contact with the electrolyte, high light adsorption efficiency enhanced by light scattering.[4] Despite such promising attributes, the overall water splitting efficiency of TNTAs photoanode falls well short of the theoretical maximum efficiency in solar radiation, which mainly ascribed to the poor spectral response in visible light for its wide band gap, low electron mobility (1 cm^2 $v^{-1}s^{-1}$),[5] and sluggish oxygen evolution reaction (OER) kinetics.[6] To date, modifying TNTAs with semiconductors nanoparticles with a narrow-band-gap such as CdS[7] or metal nanoparticle with good localized surface plasmon resonance performance such as Au[8] are often applied to sensitize TNTAs. Unfortunately, these semiconductors are not stable during the

reaction attributed to their inevitable anodic decomposition/corrosion, and the difficulty to achieve control over the nanoparticles such as their particle size and distribution on the walls of NTs and the possibility of nanoparticles to aggregate restrict their efficient use. Another active approach is doping TNTAs with appropriate anions or cations to render this material sensitive to visible light.[9] The optical absorption of TiO_2 can be effectively modified due to the electronic transitions from the dopant 2p or 3p orbitals to the Ti 3d orbits via suitable dopants. However, doping will also strengthen the recombination of photogenerated electron-hole pairs and deteriorate the photoelectric conversion efficiency of photoelectrodes.[10] Thereby, developing a suitable strategy to further enhanced PEC water splitting performance for TNTAs is still highly desirable.

The surface properties of nanomaterials are particularly important to the overall reaction efficiency because they have influence on the recombination velocity and kinetics of electrode reactions. Therefore, coating TNTAs with advanced thin films naturally comes as a rational strategy to ameliorate the surface characteristic of TNTAs. In addition, the thickness of coating film also should be optimal to reduce the negative interfering with the light absorption of TiO_2 and the number of recombination sites in the coating. Ultrathin carbon film coating inspires the idea due to their good light response and conductivity, and high stability and strength.[11] Especially, Nitrogen-doped (N-doped) carbon nanomaterials have been reported as one of best electrocatalysts for OER,[12] which will greatly enhance the OEC kinetics at the surface of TNTAs photoanode. However, plugging of the nanotubes and inhomogeneity of the coated surface often occur in traditional methods for carbon deposition, since these processes are not self-limiting.[13,14] Molecular layer deposition (MLD) is an advanced deposition method which allows growth of polymer films with molecular-level precision in a layer-by-layer manner. As a subset of atomic layer deposition, its layer-by-layer deposition allows for highly conformal coating even on

complex nanostructures.[15] Recently, George's group[16] and our group[17] respectively reported the fabricated hybrid polymer films with different MLD methods. And Putkonen et al. prepared different polyimide thin films by changing MLD parameters. [18] We also found that the obtained polymer film may be converted to carbon film via appropriate carbonization process.[19] Since the combination of polymer film can be effectively adjusted by the parameters of MLD, various functional carbon films in demand would be achieved. It appears that coating N-doped carbon films on TNTAs via MLD will turn into a promising strategy to substantially improve the PEC water splitting performance.

Herein, we show coating the interior and exterior walls of TNTAs with an ultrathin N-doped carbon film, creating a core/shell nanostructure, by combining MLD and carbonization. Core/shell nanostructures are both scientific and technological interest due to their enhanced properties compared to the single components in PEC water splitting[20]. Plugging of the nanotubes and inhomogeneity of the modified surface are avoided, and the thickness is precisely controlled by the number cycles of MLD. In addition, TNTAs was simultaneously hydrogenated in carbonization process, which will render this oxide sensitive to visible light.[21,22] The TNTAs coated with an ultrathin N-doped carbon film serve as an extraordinarily efficient and stable photoanode for PEC water splitting. This ultrathin N-doped carbon film coating is not specific of TNTAs and may be adapted to other porous photoanodes to enhance the PEC water splitting performance.

RESULTS AND DISCUSSION

Scheme 1 presents the design and preparation process of hydrogen-treated TNTAs photoanode coated with an ultrathin carbon film. Briefly, Ti foil (Scheme 1A) was electrochemically anodized and annealed in air to form TNTAs (Scheme 1B). It is imperative to maintain the structure of TNTAs during the deposition of carbon film for larger surface area and high light

absorption. Employed the MLD (Scheme 1C), core/shell nanoarrays TNTAs with an ultrathin polyimide was achieved. Subsequently, carbonization of core/shell TNTAs in H_2/Ar atmosphere (Scheme 1D) was carried out to produce an ultrathin N-doped carbon film along with the simultaneous the conversion of pristine TiO_2 to hydrogenated TiO_2, which protects and guarantees the regularity of the original morphology of TNTAs. It should be pointed out that the surface Ti^{3+} in hydrogenated TiO_2 without carbon film coating would be unstable in electrolyte since it is easily oxidized by dissolved oxygen in water.[23] The surface of coated TNTAs with an ultrathin carbon film absorbs incident light (*hv*) and produces electron-hole pairs. The holes migrate to electrode-electrolyte interface and participate in the OER. The electrons transferred to the substrate travel to the counter electrode (Pt electrode) and participate in hydrogen evolution reaction.

As shown in Figure 1, the carbon film coated TNTAs showed a similar morphology with an ordered port NT structures of the pristine TNTAs, suggesting a stable morphological structure in the coating process. The pristine TiO_2 NTs (shows a light green color) have an average wall thickness of 10 nm (Figure 1A) and length up to around 0.5 μm (Figure 1B). Using the MLD method, carbon film fully covers the surface of TiO_2 NTs (show a black color). Moreover, the smooth surface without obvious pores or cracks, is expected to prevent the electrolyte or air from contacting the surface of hydrogenated TiO_2 and improve the separation of photogenerated electron-hole pairs due to existence heterojunction interface.[24] After coating the carbon film, the average wall thickness of TiO_2 NTs increases to 16.0 nm (Figure 1C), and the thickness of carbon film with 30 MLD cycles is 3.0 nm. The length of modified TiO_2 NTs shows less difference during the preparation process, but the twist of NTs has been observed, which may stem from the influence of the applied heat treatment (Figure 1D). This length value is shorter

than the light absorption depth near the band gap (approximately 1 μm),[2] and thus guarantees an efficient light absorption.

The change of the surface state of nanomaterials can be observed by mapping their start and final states with energy-dispersive X-Ray spectroscopy (EDX)[25]. Figure 2A shows a typical SEM image of the TNTAs coated with an ultrathin carbon film. Figures 2B-E shows EDX maps of Titanium, Oxygen, Carbon, and Nitrogen, respectively. These elements are uniformly distributed on the surfaces of modified TNTAs, demonstrating high homogeneity of the obtained protective film. However, no carbon and nitrogen elements are observed on the surface of pristine TNTAs (Figure S1). This result indicates that uniform N-doped carbon film has conformally coated on the TiO_2 NTs.

Raman spectroscopy was employed to confirm the existence of ultrathin carbon film. The Raman peaks at 147, 394, 515 and 633 cm^{-1} observed in all three samples can be assigned to Eg, B1g, A1g, and Eg modes of the anatase phase, respectively, indicating the crystallinities of present TiO_2 NTs all belong to anatase TiO_2 (Figure 3A). Only in the C coating hydrogenated TiO_2 (C coating / H-TiO_2) sample, Raman analysis displays two additional bands centered around 1347 cm^{-1} and 1608 cm^{-1}, which are characteristic D band and G band for carbon materials.[26] The occurrence of G band indicates the existing of graphitized carbon in the C coating / H-TiO_2. The intensity ratio I(D)/I(G), which usually used to depict the degree of graphitization of carbon materials,[27] of the carbon film(0.42), reveals that the carbon film is well graphitized. FT-IR spectroscopy was further applied to detect potential functional groups in the carbon film. As shown in Figure 3B, only two strong peaks at 3430 (ν_{O-H}) and 631 cm^{-1}($\nu_{Ti-O-Ti}$) are found in pristine TiO_2 which could be attributed to the absorbed water molecules from air and antisymmetric Ti-O stretching, respectively. However, some new peaks between 2,850 and 2969 cm^{-1} appear in C coating / H-TiO_2 can be assigned to a methylene stretch and indicate the

existence of CH_2 or CH groups. Furthermore, the peak at 1733 cm^{-1} is attributed to carbonyl and carboxylic groups ($\nu_{C=O}$), and the peak at 1633 cm^{-1} ($\delta_{c=c}$) stems from the skeletal vibration of sp2 carbon. CO-N bending mode between 1510 and 1365 cm^{-1} and C-N stretching mode at 1265 cm^{-1} are also observed, as shown in Figure 3B. At low frequencies, two noticeable peaks are observed at 1170 cm^{-1} and 1051 cm^{-1}, corresponding with C-O vibrations. These functional groups existing in ethylenediamine and 1, 2, 4, 5-benzenetetracarboxylic anhydride will transfer to the polyimide through a condensation reaction (1). Although most of these groups are decomposed or removed in the carbonization process, some of them are still maintained in the obtained carbon film. To further confirm the element contents and states of C, O and N, X-ray photoelectron spectroscopy (XPS) analyses was carried out. As shown in Figure S2, the content of C, O and N is determined to be 81.49%, 13.79% and 4.72%, respectively (Figure S2). Moreover, only pyridine N and pyridone N at around 398.2 and 400.6 eV appear in the carbon film, which will render high electron transfer capability and electrochemical activity for carbon materials, since pyridinic nitrogen is an important active site for OER.[12]

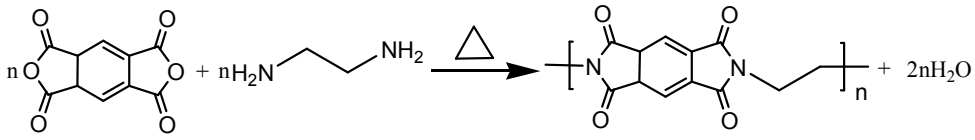

(1)

Transmission electron microscopy (TEM) and High-resolution TEM (HRTEM) investigations were conducted to further investigate the crystalline structure of carbon-film coated TNTAs. Figure 4A shows that the nanostructures have uniform diameters of about 100 nm throughout their lengths. The selected-area electron diffraction patterns (SAED, inset in Figure 4A) reveal the polycrystalline nature of these TiO_2 NTs. The observed diffraction rings agree well with the lattice spacing of anatase TiO_2 crystal. A typical lattice-resolved TEM image collected from a

small NT (Figure 4B) reveals that two clear amorphous carbon film were uniformly deposited on the interior and exterior walls of NTs, respectively, identifying a core/shell nanostructure. So it is clear that dense carbon film has conformally coated the walls of TiO_2 NTs. In contrast, no carbon film was observed on HRTEM image of pristine TiO_2 (Figure S3). Figure 4C shows the interplanar spacing of 3.52 Å and 2.38 Å matches well the (101) and (004) plane of anatase TiO_2 (JCPDS 89-4921). The precisely control of the thickness of carbon film could be achieved by varying the number of MLD cycles. For example, the average carbon thickness determined by HRTEM are 0.92, 2.78, and 5.18 nm after 10, 30, and 50 cycles, respectively (Figure 4C-E). The thickness of the carbon film linearly increased with MLD cycles (Figure 4F) at a growth rate of 1.03 Å /cycle. It is worth to mention that C coating/H-TiO_2 for less than 5 cycles has some cracks on the carbon surface (See Figure S4), which will deteriorate the stability of modified TNTAs. Thus, choosing the TNTAs with 10, 30, 50 coating cycles in this manuscript is applied. XRD patterns were collected to determine the crystal and possible phase changes during the preparation process. The pure anatase phase of TiO_2 was found in pristine TiO_2 NTs as confirmed in Figure S5, However, the low ratio rutile phase TiO_2 emerges in H-TiO_2 and C coating/H-TiO_2 due to the heat treatment. Moreover, the diffraction peak at 2θ of 42.1^o, which corresponded to the graphite crystal face of (100), was detectable only in the C coating/H-TiO_2 sample, corresponded well with HRTEM characterization. Good graphitization of carbon film will give strong electron-transfer ability to TNTAs.

The optical absorption properties of the three samples were measured using UV-vis absorption spectroscopy and were shown in Figure 5A. It is clear that the band gap of the pristine TiO_2 is calculated to be 3.19 eV according to the formula $Eg=1240/\lambda$.[28] The light absorption edges of hydrogenated TiO_2 samples extend from ultraviolet to visible due to the formations of intraband transitions in hydrogenation at high temperature.[21] Thereby visible light is also able to be

captured to generate carriers for photoelectrochemical reactions. In addition, no decreased absorption in the short wavelength region from 320 to 400 nm was found after carbon coating, indicating the N-doped carbon film does not reduce the light absorption of TiO_2 NTs. Compare to the H-TiO_2, an obviously enhanced absorbance for C coating/H-TiO_2 TNTAs in visible light is observed due to the strong absorption of carbon in this region.

A preliminary (proof-of-concept) PEC performance measurements were carried out in a home-made three electrode electrochemical cell (Shown in Figure S6). The dependences of photocurrent density on applied potential ($J-V$) plots in the dark and under AM 1.5 G illumination were shown in Figure 5B. All electrodes show negligible current values in the dark over the displayed potential range. The onset photocurrent potentials for pristine TiO_2 sample appears at ~−0.8 V versus Ag/AgCl, which is agree well with the reported value (~−0.84 V versus Ag/AgCl) for TiO_2 electrodes in 1 M KOH electrolyte.[29] After hydrogenation and carbon coating, this value shifted to around −0.9 V, which indicates a shift in Fermi level to more negative potential,[30] demonstrating a better charge separation and electron accumulation in C coating/H-TiO_2 than that in H-TiO_2 and pristine TiO_2. All photoelectrodes display a continuously increasing photoresponse with increasing bias potential. However, C coating/H-TiO_2 photoelectrode displays a much superior activity to the H-TiO_2 and pristine TiO_2 photoelectrode over the whole examined bias range. The highest photocurrent density of C coating/H-TiO_2 photoelectrode with 10 MLD cycles at 0 V versus Ag/AgCl could be achieved to be 3.6 mA cm^{-2}, which is 1.6 times larger than that of H-TiO_2 electrode and 5.4 times larger than that of pristine TiO_2. Moreover, the value of 3.6 mA cm^{-2} is still higher than the value of other reports about TNTAs modified with other carbon materials.[13,14,] Basically, thinner walls benefit the charge transport in TNTAs according to Grimes's report.[31] In our case, the thickness of walls in TNTAs modified with carbon film deposition for 10 MLD cycles is thinnest, and the defects in this

carbon film which are the active sites for recombination of photogenerated electrons-hole pairs is also least. In addition, when the cycle number is less than 10, there are some cracks on the carbon film. These racks will deteriorate the electro-transfer capability of the carbon film, which strengthens the recombination of photo-generated electrons-hole pairs, and reduces the PEC performance. Therefore, TNTAs photoelectrode with 10 cycles of carbon film coating exhibits the best PEC performance. In the coming part, only TNTAs photoelectrode with 10 cycles of carbon film coating was investigated in detail due to its best PEC performance.

To evaluate the performance of photoanode, the photoresponses of three samples were investigated by chronoamperometric (photocurrent versus time) (*J*-*t*) curves measurements under pulsed illumination at a constant potential of 0.23 V versus Ag/AgCl, because it corresponds to the water oxidation potential. As shown in Figure 5C, the photocurrent values of all electrodes decreased to nearly zero as soon as the incident light on the photoanodes was turned off and had a transient increase only when the light was turned on again., These results reveal that that all of these electrodes have fast photoresponses. However, the H-TiO_2 photoanode shows a rapid decrease at the first few cycles, which could be contributed to the oxidation of surface-doped Ti^{3+} and the wall rupture in TiO_2 NTs without carbon film coating in annealing (See Figure S7). However, after coating the TiO_2 NTs with carbon film, the oxidation of Ti^{3+} and structural rupture could be prevented and thus, no rapid decrease was observed (Figure 1D,5C).Moreover, although the C coating/H-TiO_2 photoanode shows that the stable-state current decay, the rate is much slower than that of pristine TiO_2 photoanode. This result indicated that TiO_2 NTs coated with carbon film possess good tolerance against photocorrosion and have a potential long-term application as photoanode in PEC water splitting.

Furthermore, incident-photon-to-current conversion efficiency (IPCE) measurements which were performed at a constant potential of 0.23 V vs Ag/AgCl, were utilized to estimate the

wavelength-dependent light harvesting efficiency. IPCE values can be calculated using the following equation:[22]

$$IPCE=(1240I) / (\lambda J_{light}) \quad (2)$$

where I is the photocurrent density (mA cm^{-2}), J_{light} is the incident light irradiance (mW cm^{-2}), and λ is the incident light wavelength (nm). As shown in Figure 5D, the C coating/ H-TiO_2 sample exhibits significantly increases in photoactivity in the range from 300 to 500 nm wavelength compared to the pristine TiO_2 and H-TiO_2. For example, C coating/H-TiO_2 has the IPCE value of 64.5% at 330 nm, which is 1.7 times higher than that of H-TiO_2 sample and 4.8 times higher than that of pristine TiO_2 sample. Moreover, the IPCE values of C coating / H-TiO_2 shows t a small peak at 440 nm, which is direct evidence for a visible photoresponse. IPCE results for all the photoanodes are also consistent with their corresponding *J-V* characteristics. The enhanced performance might be attributed to the fact that the coating carbon films on the walls of TNTAs forms a core/shell nanostructure, where the herterojunction can act as an energy barrier to suppress the recombination of photogenerated electron-hole pairs, and the electron transporting carbon film shell simultaneously strength the reactivity of photogenerated hole for water splitting.[24,32]

To further understand the enhanced PEC performance, the inherent electronic properties of TNTAs were characterized by measuring the onset OER potential, linear Tafel plots and electrochemical impedance spectroscopy (EIS). It is well-known that the larger overpotential of TiO_2 for OER, presenting the sluggish kinetics, commonly limits its wide application in PEC water splitting. The onset potential for OER of pristine TiO_2, H-TiO_2 and C coating/H-TiO_2 is 0.583, 0.599, and 0.539 V, respectively, and thus, the overpotential of TiO_2 for OER showed a general order of $\Delta_{H\text{-}TiO2}>\Delta_{pristine\ TiO2}>\Delta_{C\ coating/H\text{-}TiO2}$. This lower overpotential of C coating / H-TiO_2 suggests that electrocatalytical activity in TNTAs was greatly enhanced by the N-doped

carbon coating. However, the electrocatalytical activity could be deteriorated by hydrogen treatment. As mentioned above in XPS results, pyridinic-nitrogen-or/and quaternary-nitrogen-related sites were formed in the obtained N-doping carbon film. Thus the carbon atoms adjacent to nitrogen atoms would be positively charged due to the electron-withdrawing nitrogen atoms in a graphene π-system,[33] which can facilitate the absorption of OH^- and support the easy recombination of two O_{ads} additives. In addition, N-doping in carbon materials could also increase the electron transfer capability to reduce Ohmic polarization.[34] Therefore, the N-doped carbon film displays a low overpotentials for OER, and thus remarkable enhance the OER kinetics. However, the surface of H-TiO_2 become more hydrophobic due to hydrogen passives the dangling bonds of TiO,[20] which results in the interactions of the absorbed species (such as OH-, H_2O, and O_{ads}) on the surface of H-TiO_2 rapidly decreased. Thus a high overpotential for OER in H-TiO_2 was observed.

Basically, the Tafel plot describes the relationship between the overpotential (η) and the logarithm of the current (ik), which is the important metrics for water oxidation electrocatalysts and can provide important information about electronic and geometric enhancement in activity for electrocatalysts.[35] In general, a decrease in the slope of the curve is representative of a beneficial electronic effect. Similarly, an increase in the exchange current (or the intercept of the line with the potential axis) is the result of a beneficial geometric effect or an enhanced surface area. As shown in Figure 6, the slope of the Tafel curve for pristine TiO_2, H-TiO_2 and C coating/H-TiO_2 is 82, 104, and 67 mV/ decade, respectively. In addition, the exchange current showed a general order of $Io_{\text{C coating/H-TiO2}} > Io_{\text{H-TiO2}} > Io_{\text{pristine TiO2}}$. Obviously, the C coating / H-TiO_2 sample exhibits the lowest slop value and the biggest exchange current value. These results demonstrate that the electronic and geometric effect on the surface of TNTAs could be simultaneously ameliorated via the ultrathin carbon coating.

Figure 6C presents Nyquist plots measured by electrochemical impedance spectroscopy (EIS) under illumination (Nyquist plots in the dark shown in Figure S8). All of the photoelectrodes show two semicircles. However, the semicircle at low-frequency is greatly reduced in the C coating/H-TiO_2 based photoelectrode..Usually, the semicircle at high-frequency zone presents the diffusion of ions in NTs, which is typical EIS character of the embedded electrode, and the low-frequency semicircle which is equal to the charge transfer resistance (Rct) is the characteristic of the charge transfer process.[36] The C coating/H-TiO_2 showed a lower Rct value than that of H-TiO_2 and pristine TiO_2 both in the dark and under illumination. This result suggests the N-doped carbon film could accelerate charge transfer kinetics and act as a high effective water oxidation electrocatalyst. This is benefit for the PEC water splitting performance of TNTAs photoanode.

Moreover, the capability of charge separation via carbon coating can be verified by the photoluminescence (PL) spectroscopy.[37] As shown in Figure 6D, a broad-band emission around 410 nm wavelength (excited at 325 nm) appears which can be attributed to the recombination of photoexcited holes with electrons occupying the singly ionized oxygen vacancies in TiO_2.[38] High PL intensity presents high level of the recombination of photogenerated electron-hole pairs. Compared to that of H-TiO_2 /pristine TiO_2, the PL intensity for C coating/H-TiO_2 decreases significantly, indicating superior performance for impeding photogenerated charge recombination, which could attributed to carbon coating may passivate the surface state of TiO_2 and the carbon film would facilitate the electron transfer from electrolyte to TNTAs photoanode in C coating/ H-TiO_2 sample.

CONCLUSION

In conclusion, a uniform ultrathin N-doped carbon film coating on the interior and exterior walls of hydrogen-treated TNTAs was achieved through a MLD strategy. The formed core/shell

nanostructures not only enhance the stability of hydrogen-treated TNTAs via carbon coating, but also improve the separation of photogenerated electron-hole pairs due to the existence of heterojunction interface. Simultaneously, hydrogenation extends the absorption spectrum from UV to visible light. Moreover, highly active N-doped carbon film greatly improves the kinetics of PEC water splitting, and leads to the applied potential required to drive photo-assisted water splitting shifted cathodically by 100 mV. Therefore, the 5-fold increases in the photocurrent and enhanced photostability of C coating/ H-TiO_2 under AM1.5G light illumination as compared pristine TiO_2, was obtained. This combination of enhanced photocatalytic activity and photostability makes ultrathin N-doped carbon film coating a promising strategy in the fields of PEC water splitting for TNTAs or other porous semiconductors.

METHODS

Preparation of TNTAs. Highly ordered TNTAs were fabricated through anodic oxidation of Ti substrates. Before the anodization, Ti substrate was chemically etched by immersing it in a mixture of 40% HF, HNO_3 and deionized water (HF: HNO_3 :H_2O=1:4:5 in volume). Then the Ti foil was ultrasonically washed in acetone and ethanol for 5 min each. The cleaned Ti foil was anodized in a 0.5% HF electrolyte in a two-electrode cell with the Ti foil as the working and a plate sheet as the counter electrode in an ice bath under the assistance of magnetic stirring. The potentiostatic anodic oxidation was performed under 25 V for 40 min. After sonication for 5 mins, the sample was put in a muffle furnace under oxygen atmosphere with flow rate of 60 sccm, then heated to 500°C with a rate of 3 °C min^{-1} and maintained at the temperature for 2 hours. Then it was cooled to room temperature with rate of 3 °C min^{-1}. Finally a plate of pristine TNTAs was achieved.

Coating TNTAs with ultrathin carbon films by MLD. The MLD of polyimide on TNTAs was carried out in a home-made, closed type, hot wall ALD reactor. The pristine TNTAs plate was transferred to the ALD chamber for the growth of carbon ultrathin film. The deposition was carried out with ethylenediamine (EDA) and 1, 2, 4, 5-benzenetetracarboxylic anhydride (PMDA) as precursorss using N_2 as a carrying gas. The deposition temperature was 165 °C while EDA and PMDA were kept at room temperature and 150 °C, respectively. The obtained TNTAs plate modified with polyimide film was then transferred into a quartz tube furnace and annealed at 600 °C for 1 h in H_2/Ar gas flow to produce ultrathin carbon films.

Characterization of Catalysts. Raman spectra of the samples were collected on a Horiba Labram HR800 spectrometer with an excitation wavelength of 633 nm. FTIR spectroscopy was recorded with a Bruker Tensor 27 spectrometer. The chemical composition and bonding configurations were evaluated by X-ray photoelectron spectroscopy (XPS) performed on a Kratos XSAM 800 spectrometer using Al Kα (hk = 1486.6 eV) X-ray source. The crystalline structures were characterized by X-ray diffraction (XRD, Rigaku D / MAX-rA, Japan) using a diffract meter with Cu Kα radiation, $\lambda = 1.54184$ Å in the range of $2\theta = 15 \sim 75^{o}$ at a scan rate of 4^{o} min^{-1}. Field emission scanning electron microscopy (FE-SEM) on a Hitachi S-4800 microscope was applied to observe the morphologies of ultrathin carbon modified TNTAs. The transmission electron microscopy (TEM) images were obtained by using a JEOL-2100F microscope. A U-3900 spectrophotometer was employed for measuring the UV-vis absorption spectra of ultrathin carbon modified TNTAs. Photoluminescence measurement was carried on a Hitachi F-7000 spectroscopy.

Photoelectrochemical measurement. The electrochemical and photoelectrochemical properties of each sample were tested using a three electrode electrochemical cell with a Ag/AgCl reference electrode (3 mol L^{-1} KCl filled) and Pt plate (1.5 cm×1.5 cm) counter

electrode with CHI760D electrochemical workstation. The working electrode (the photoanode consisting of the ultrathin carbon film modified TNTAs) with illuminated area 1.50 cm^2 was immersed in 1 M KOH and illuminated using a 300 W xenon lamp with a light intensity of 100 mW cm^{-2} (PLS-SXE300, PE300BF) coupled with an AM 1.5G filter used as the solar light. Linear sweep voltammetry was performed with a voltage scan speed of 5 mVs^{-1}, and the light was chopped manually at regular intervals at a fixed potential of 0.23 V vs Ag/AgCl. . Electrochemical impedance spectra were measured by applying a bias of 0.23 vs Ag/AgCl over the frequency range of 10^{-1} to 10^5 Hz with a 5 mV amplitude under at 100 mW cm^{-2} illumination. A monochromator (Oriel) was also employed to study spectral response and was used in conjunction with a power meter and photodiode (Newport) to calculate IPCE. The IPCE was measured as a function of wavelength from 300 to 500 nm with three-electrode configuration under 0.23 V vs Ag/AgCl.

Conflict of Interest: The authors declare no competing financial interest.

ACKNOWLEDGMENT. X.T. greatly acknowledge financial support from Shanxi Province Science Foundation for Youths (2013021011-6). Y. Q. acknowledges financial support from Research Project Supported by Shanxi Scholarship Council of China (2013-152), the Hundred Talent Programs of the Chinese Academy of Sciences, and the Hundred Talent Programs of Shanxi Province. We thank P. Li and X. Ao for helpful discussions.

Supporting Information Available. Additional figures and experimental details are included. "This material is available free of charge *via* the Internet at http://"

NOTES AND REFERENCES

1, A. Fujishima, and K. Honda, *Nature,* **1**972, **238**, 37-38.

2, Z. Zhang, and P. Wang, *Energy Environ.Sci.*, 2012, **5**, 6506-6512.

3, F.F.Abdi, L.Han, A.H.M Smets,. M.Zeman, B.Dam, and R.V.D. Krol, *Nat. Commun.,* 2013, DOI:10.1038/ncomms3195.

4, P.Roy, S. Berger, and P. Schmuki, *Angew. Chem. Int. Ed.,* 2011, **50**, 2904-2939.

5, E. Hendry, M. Koeberg, B. O'Regan, and M. Bonn, *Nano Lett*., 2006, **6**, 755-759.

6, B. Liu, H. M. Chen, C. Liu, S.C. Andrews, C. Hahn, and P. Yang, *J. Am. Chem. Soc.,* 2013, **135**, 9995-9998.

7, W. Zhu, X. Liu, H. Liu, D. Tong, J. Yang, and J. Peng, *J. Am. Chem. Soc.,* 2010, **132**, 12619-12626.

8, Z. Zhang, L. Zhang, M.N. Hedhili, H. Zhang, and P. Wang, *Nano Lett*., 2013, **13**, 14-20.

9, R. Asahi, T. Morikawa, T. Ohwaki, K. Aoki, and Y.Taga, *Science,* 2001, **293**, 269-271.

10, Q. Kang, J. Cao, Y. Zhang, L. Liu, H. Xu, and J. Ye, *J. Mater. Chem. A,* 2013, **1**, 5766-5774.

11, J. Deng, X. Lv, J. Gao, A. Pu, M. Li, X. Sun and J. Zhong, *Energy Environ.Sci.*, 2013, **6**, 1965-1970.

12, Y. Zhao, R. Nakamura, K. Kamiya, S. Nakanishi, and K. Hashimoto, *Nat. Commun*., 2013, DOI:10.1038/ncomms3390

13, P. Song, X. Zhang, M. Sun, X. Cui, and Y. Lin, *Nanoscale,* 2012, **4**, 1800-1804.

14, X. Zhou, F. Peng, H. Wang, H. Yu, and Y. Fang, *Chem. Commun.* 2011, **47**, 10323-10325.

15, M. Knez, K. Nielsch, and L. Niinistö, *Adv. Mater.*, 2007, **19**, 3425- 3438.

16. A. I. Abdulagatov, R. A. Hall, J. L. Sutherland, B. H. Lee, A. S. Cavanagh, and S. M. George, *Chem. Mater.,* 2012, **24**, 2854-2863.

17, C.Q. Chen, P. Li, G.Z. Wang, Y. Yu,; F.F,.Duan, C.Y. Chen, W.G Song, Y. Qin, and M. Knez, *Angew. Chem. Int. Ed.,* 2013, **52,** 9196-9201.

18, M. Putkonen, J. Harjuoja, T. Sajavaara, and L. Niinisto, *J. Mater. Chem.,* 2007, **17**, 664-669.

19, P. Yang, G. Wang, Z. Gao, H. Chen, and Y. Qin, *Materials,* 2013, **6**, 5602-5607.

20, C.Yang, Z. Wang, T. Lin, H. Yin, X. Lu, D. Wan, T. Xu, C. Zheng, J. Lin, F. Huang, X. Xie, M. Jiang, *J. Am. Chem. Soc*., 2013, **135**, 17831−17838.

21, X. Chen, L. Liu, P.Y. Yu, and S.S. Mao, *Science,* 2011, **331**, 746-750.

22, G. Wang, H. Wang, Y. Ling, Y. Tang, and X. Yang, *Nano Lett.,* 2011, **11**, 3026-3033.

23, K. Komaguchi, T. Maruoka, H. Nakano, I. Image, Y. Ooyama, and Y. Harima, *J. Phys. Chem. C,* 2010, **114**, 1240-1245.

24, Y. Lin, S. Zhou, X. Liu, S. Sheehan, and D. Wang, *J. Am. Chem. Soc*., 2009, **131**, 2772-2773.

25, J. Seo, I. Jeon, J. Baek, *Chem. Sci.*, 2013, **4**, 4273–4277.

26, K.N. Kudin, B. Ozbas, H.C. Schniepp, R.K., Prud'homme, I.A. Aksay, and R. Car, *Nano Lett.,* 2008, **8**, 36-41.

27, S.J. Pastine, D. Okawa,; B. Kessler, M. Rolandi, M. Llorente, A. Zettl, and J. M. J. Frechet, *J. Am. Chem. Soc.,* 2008, **130**, 4238-4239.

28, P. Ji, J. Zhang, F. Chen, and M. Anpo, *J. Phys. Chem. C*, 2008, **112**, 17809-17813.

29, Q. Peng, B. Kalanyan, P. G. Hoertz, A. Miller, D. H. Kim, K. Hanson, L. Alibabaei, J. Liu, T.J. Meyer, G.N. Parsons, and J.T. Glass, *Nano Lett*., 2013, **13**, 1481-1488.

30, N. K. Allam, A. J. Poncheri, and M. A. El-Sayed, *ACS Nano,* 2011, **5**, 5056-5066.

31, C. Grimes, and G.K. Mor, TiO_2 Nanotube Arrays: Synthesis, Properties, and Applications, Springer Verlag, **2009**.

32, S. K. Karuturi, J. Luo, C. Cheng, L. Liu, L.T. Su, A.L.Y. Tok, and H. J. Fan, *Adv. Mater.,* 2012, **24**, 4157-4162.

33, H. Kim, K. Lee, S.I. Woo, and Y. Jung, *Phys. Chem. Chem .Phys*., 2011, **13**, 17505–17510.

34, D. H. Lee, W.J. Lee, and S.O. Kim, *Nano Lett*., 2009, **9**, 1427-1432.

35, J. Moir, N. Soheilnia, P. O'Brien, A. Jelle, C.M. Grozea, D. Faulkner, M.G. Helander, and G.A. Ozin, *ACS Nano*, 2013, **7**, 4261-4274.

36, S. C. Riha, B.M. Klahr, E.C. Tyo, S. Seifert, S. Vajda, M.J. Pellin, T.W. Hamann, and A. B. F. Martinson, *ACS Nano,* 2013, **7**, 2396-2405.

37, N. Zhang, S. Liu, X. Fu, and Y. Xu, *J. Phys. Chem. C,* 2011, **115**, 9136-9145.

38, M. Ye, J. Gong, Y. Lai, C. Lin, and Z. Lin, *J. Am. Chem. Soc.*, 2012, **134,** 15720-15723.

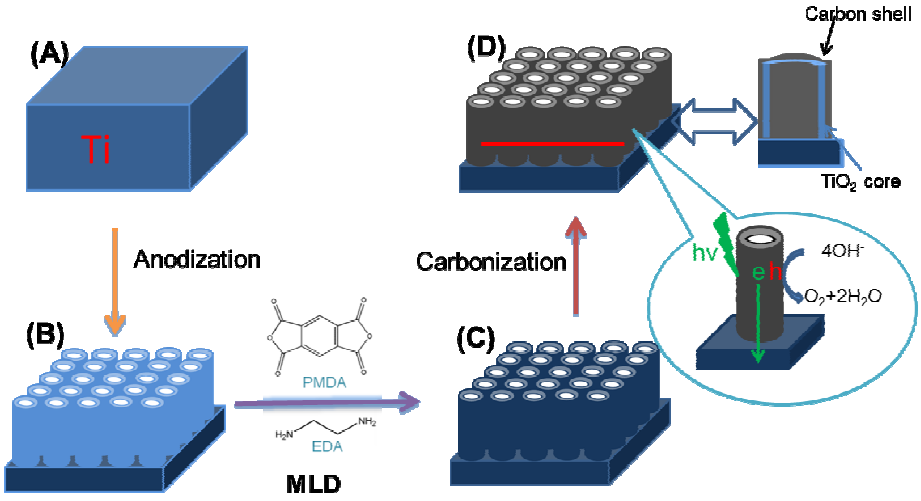

Scheme 1. Schematic illustration of the coating of TNTAs with an ultrathin carbon film: (A) Ti foil, (B) Anodized TNTAs, (C)the MLD of polyimide on TNTAs, (D) ultrathin carbon coating/TNTAs core/shell structure. Photons (hv) are absorbed by the sensitization film, producing electron-hole (e-h) pairs. The holes travel only short distances to reach the electrolyte. The electrons are conducted through the core material to the conducting substrate.

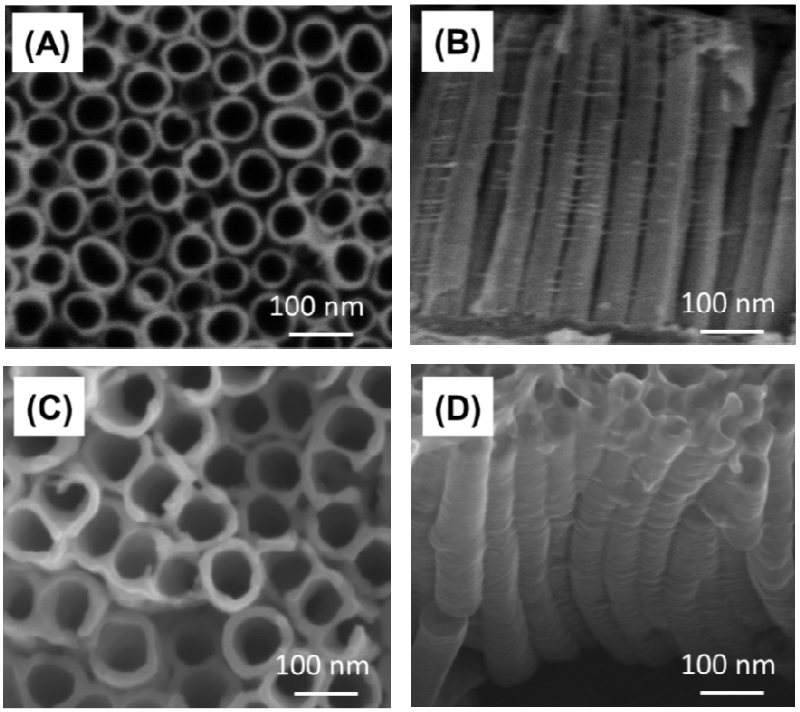

Figure 1. FE-SEM morphorogies of the TNTAs film: (A) a typical top view and (B) a cross-sectional view of pristine TNTAs; (C) a typical top view and (D) a cross-sectional view of TNTAs coated with carbon film by MLD with 30 cycles.

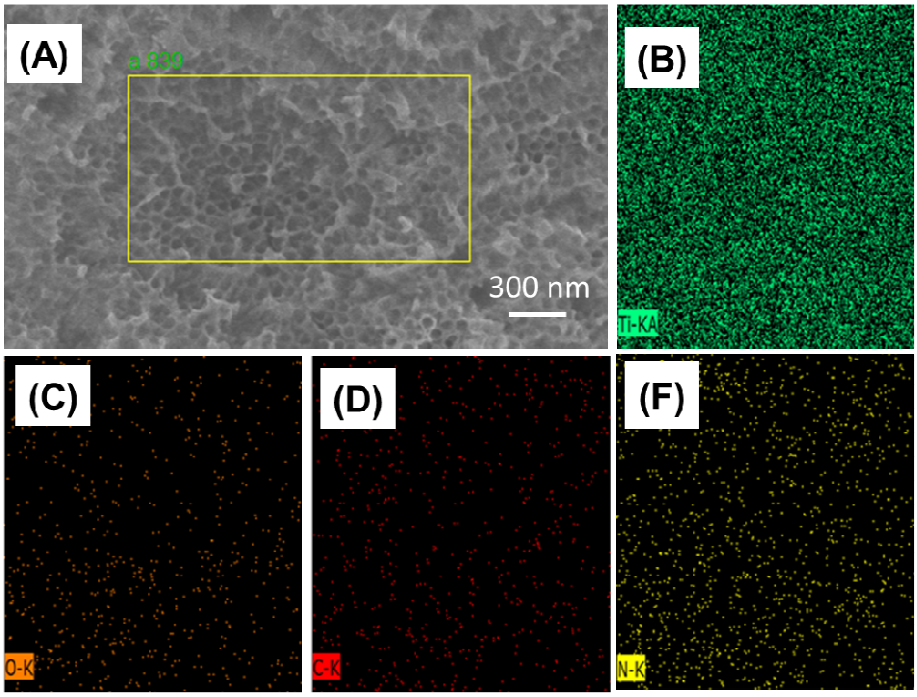

Figure 2. Element analysis of a modified TNTAs via MLD for 30 cycles, (A) the SEM image of the modified TNTAs. (B-E) Elemental maps of the boxed areain (A) for Ti, O, C, and N, respectively.

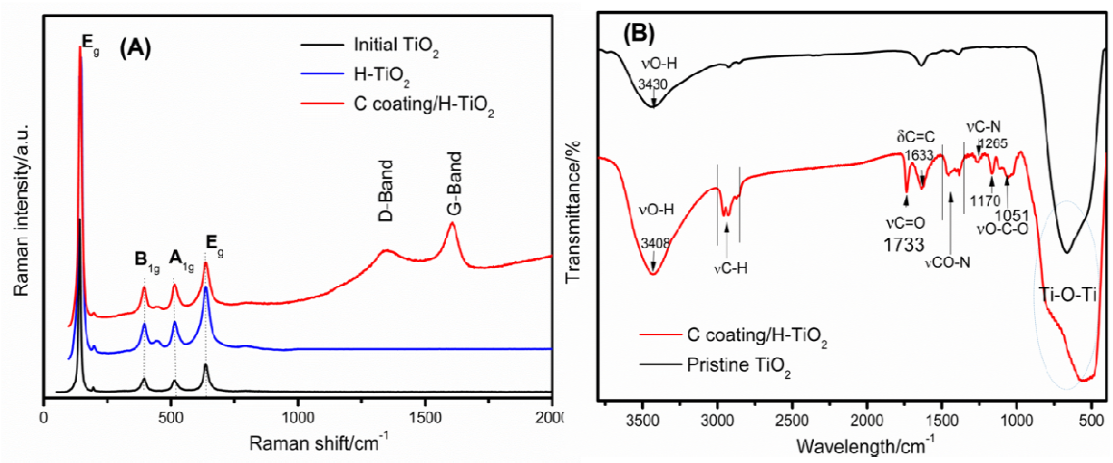

Figure 3. (A)The Raman and (B) Infrared spectra of pristine TiO_2 (black line), H-TiO_2 (blue line) and C coating/H-TiO_2 (red line).

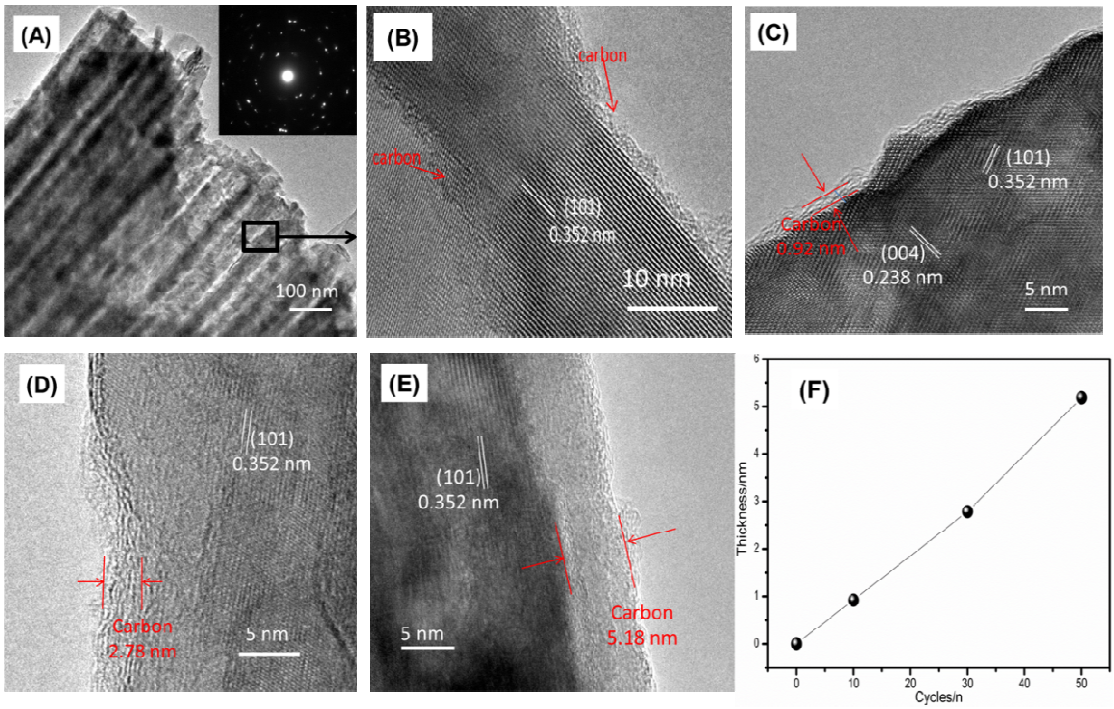

Figure 4 (A)TEM image of TNTAs coated carbon film (inset : corresponding SAED pattern), (B) Image of the boxed region in (A) at higher magnification showing the (101) planes of anatase TiO_2.HRTEM images of carbon film on the walls of TiO_2 NTs by MLD with (C) 10, (D) 30, and (D) 50 cycles.(F) the thickness of carbon film were plotted vs MLD cycles, showing that the growth rate is linear.

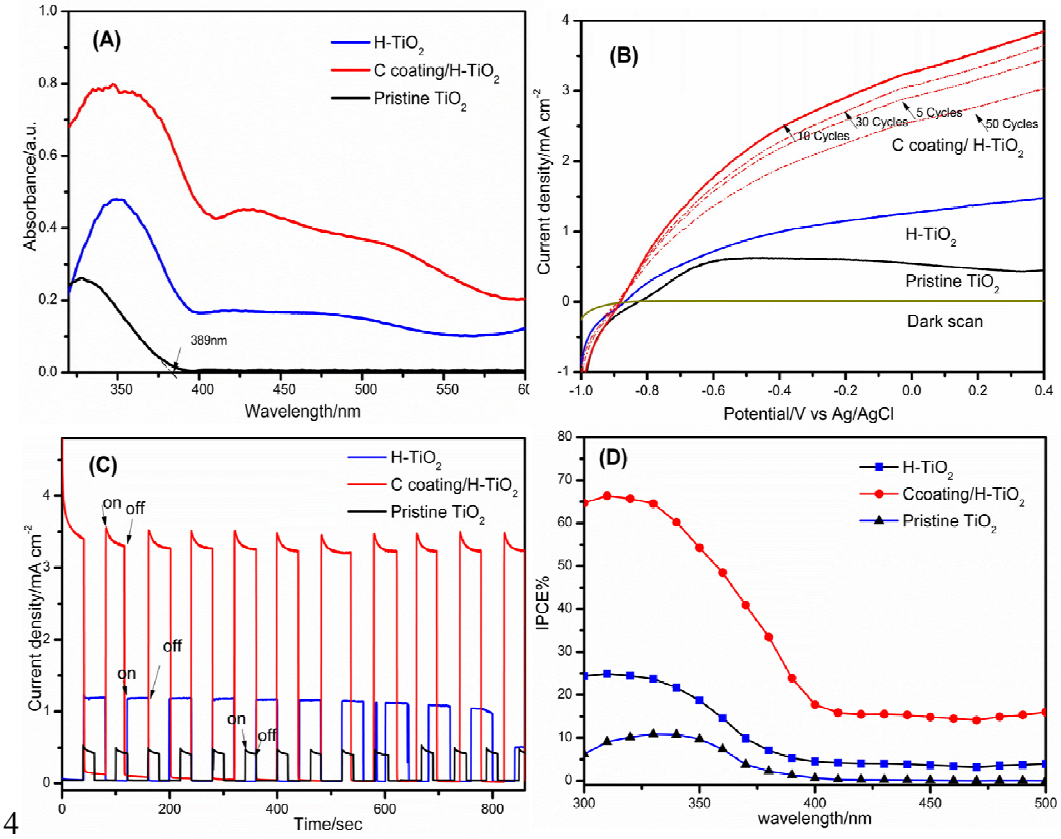

4

Figure 5. (A) UV-vis absorbance spectroscopy, (B) Linear sweep voltammetry measurements, (C) Chronoamperometric *J-t* curves at an applied potential of 0.23 V vs AgCl/Ag under illumination with light on/off cycles, and (D) IPCE spectroscopy at 0.23 V vs AgCl/Ag of pristine TiO_2 (black line), H-TiO_2 (blue line) and C coating/H-TiO_2 (red line).

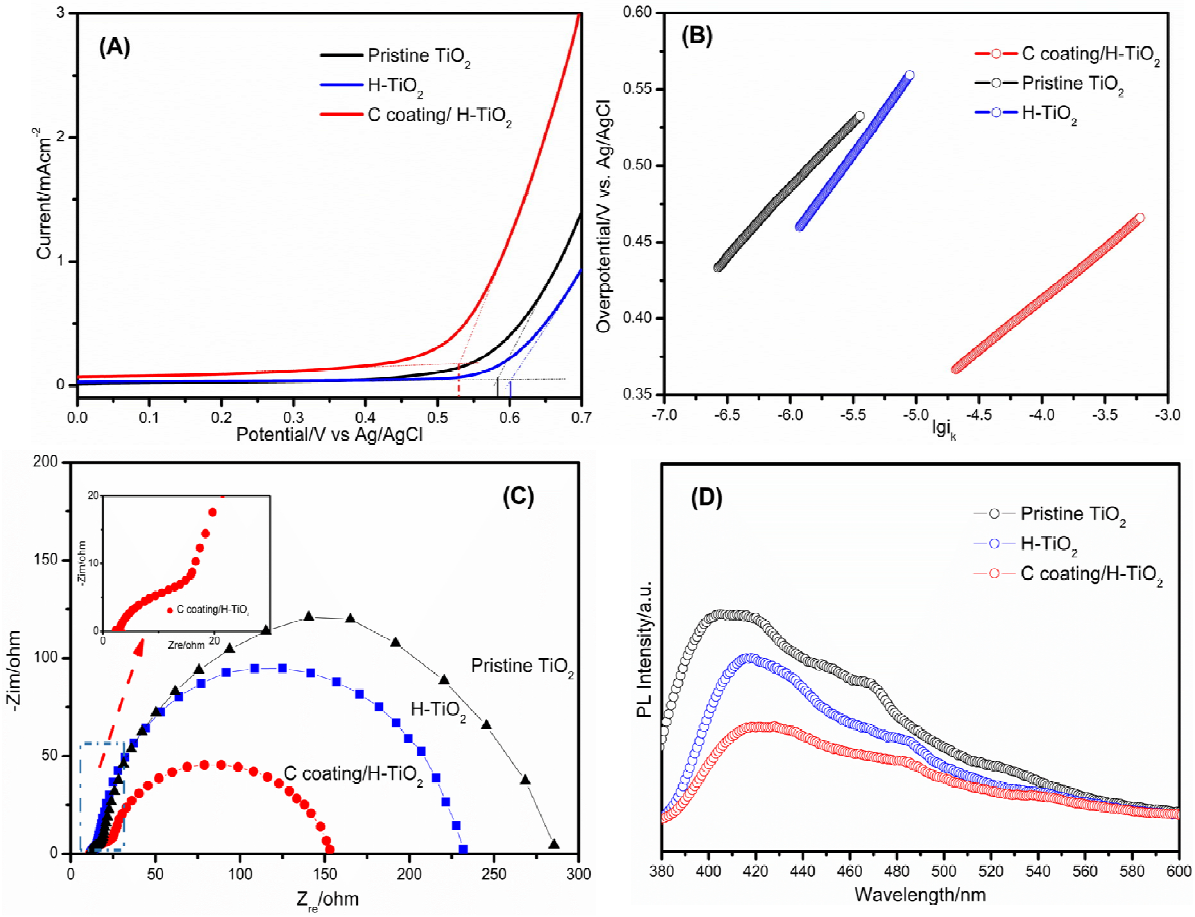

Figure 6. (A) Onset potential measurement for oxygen evolution reaction (OER), (B) Linear Tafel plots, (C) Electrochemical impedance spectroscopy of Nyquist plots at an applied potential of 0.23 V vs AgCl/Ag under 100 mW cm^{-2} illumination, and (D) Photoluminescence (PL) spectroscopy of pristine TiO_2 (black line), H-TiO_2 (blue line) and C coating/H-TiO_2 (red line).

TOC graphic

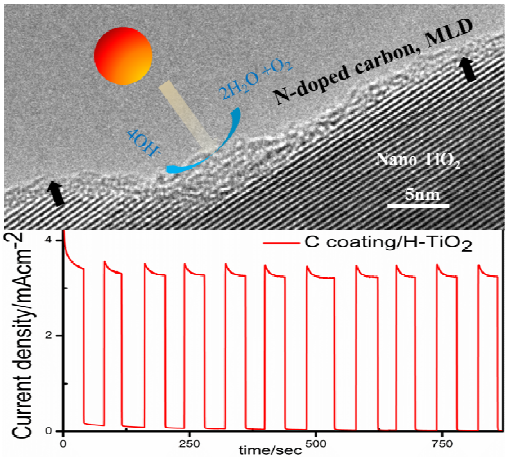

TiO_2 nanotube arrays coated carbon film by MLD exhibit excellent capability for PEC water splitting with optimized the carbon-film thickness.